IOPscience iopscience.iop.org

Home Search Collections Journals About Contact us My IOPscience

Spin waves and the critical behaviour of the magnetization in $MnPS_3$

This content has been downloaded from IOPscience. Please scroll down to see the full text.

1998 J. Phys.: Condens. Matter 10 6417

(http://iopscience.iop.org/0953-8984/10/28/020)

View the table of contents for this issue, or go to the journal homepage for more

Download details:

IP Address: 142.58.129.109
This content was downloaded on 05/06/2015 at 14:39

Please note that terms and conditions apply.

J. Phys.: Condens. Matter **10** (1998) 6417–6428. Printed in the UK PII: S0953-8984(98)90593-8

Spin waves and the critical behaviour of the magnetization in $MnPS_3$

A R Wildes†‡, B Roessli§, B Lebech‖ and K W Godfrey†

† Clarendon Laboratory, University of Oxford, Parks Rd, Oxford, UK

‡ Institut Laue–Langevin, BP 156, 38042 Grenoble Cédex 9, France¶

§ Laboratory for Neutron Scattering, ETH Zurich and Paul Scherrer Institute, 5232 Villigen, Switzerland

‖ Condensed Matter Physics and Chemistry Department, Risø National Laboratory, DK-4000 Roskilde, Denmark

Received 30 December 1997, in final form 15 May 1998

Abstract. Inelastic neutron scattering from a single crystal of the quasi-two-dimensional antiferromagnet $MnPS_3$ has been used to measure the spin wave dispersion curve at 4 K. The exchange integrals were subsequently calculated from linear spin wave theory. The values $J_1 = -0.77$ meV, $J_2 = -0.07$ meV, $J_3 = -0.18$ meV and $J' = 0.0019$ meV are within stability conditions calculated from mean-field theory. In addition, the critical behaviour of the gap in the spin wave energy at the Brillouin zone centre has been measured, and compared to the critical behaviour of the magnetization from neutron scattering data of the magnetic (020) Bragg peak. The gap varies with magnetization for $T < 0.96\ T_N$, and with the square of the magnetization for $T > 0.96\ T_N$. Two possible explanations are proposed: a competition between single-ion and dipolar anisotropies; or a crossover to XY-like excitations.

1. Introduction

There have been many studies of the quasi-low-dimensional MPX_3 systems (M = transition metal; X = S, Se) in a wide variety of research fields. These materials are quasi-two-dimensional atomically and magnetically, with layer planes held together by van der Waals forces. The low-dimensional magnetic nature makes these materials of interest for the studies of phase transitions and critical excitations. An added point of interest in these studies is that the weak interplanar atomic bonding allows easy intercalation into these compounds of a wide variety of materials; including lithium and many organic molecules. Intercalation has a dramatic effect on the magnetic and critical properties of these materials; however before these effects can be fully understood it is necessary to understand the nature of these properties in the parent material.

$MnPS_3$ is an example of these systems. It is monoclinic, with the $C2/m$ space group. The lattice parameters have been determined to be $a = 6.077$ Å, $b = 10.524$ Å, $c = 6.798$ Å, and angle $\beta = 107.35°$ (Ouvrard *et al* 1985) with the Mn atoms in (4g) sites, the P atoms in (4i) sites and the S atoms in (4i) and (8j) sites. The magnetic susceptibility of this material is best described by a two-dimensional Heisenberg model, and as such $MnPS_3$ should not order at a finite temperature. In reality, it orders into an antiferromagnetic structure below the Néel temperature of 78 K. This structure was first determined using neutron powder

¶ Current address.

 © 1998 IOP Publishing Ltd

diffraction by Kurosawa *et al* (1983). The magnetism is due to the $S = 5/2$ manganese atoms, which lie in a honeycomb arrangement in the ab planes. In the ordered state, the moments on the manganese atoms align perpendicularly to these planes. Figure 1(a) shows the atomic structure and figure 1(b) the magnetic structure.

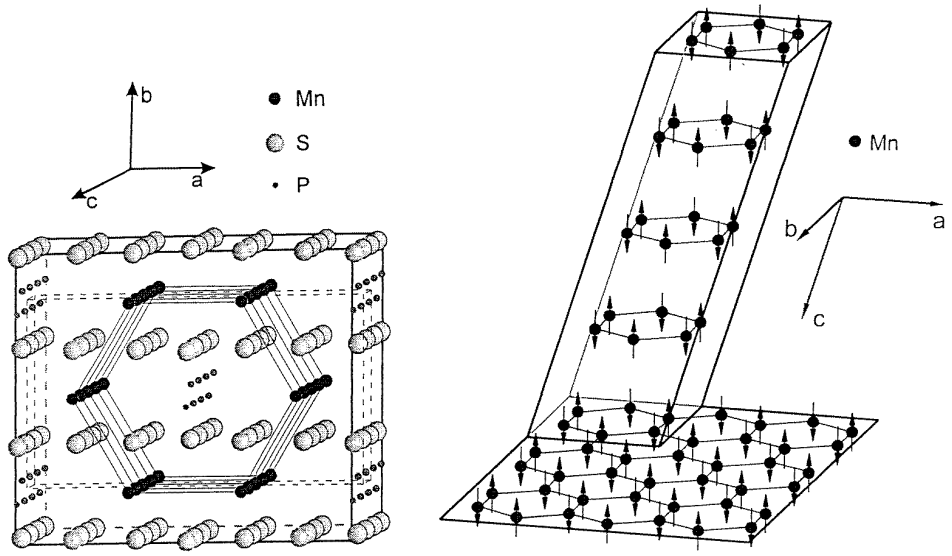

(a) (b)

Figure 1. Atomic (a) and magnetic structure (b) of $MnPS_3$. In (a), the structure is viewed with the c-axis almost perpendicular to the paper, but turned 2 degrees around the a-axis and 1 degree around the b-axis for illustrative purposes. The dashed lines in (a) shows the crystallographic unit cell. In (b), the structure is viewed with the b-axis almost perpendicular to the paper, but turned 15 degrees around the c-axis and 15 degrees around the a-axis for illustrative purposes. Part of this diagram was produced with ATOMS, by Shape Software.

The magnetic properties have been investigated by many experimental techniques such as magnetic susceptibility, electron paramagnetic resonance (Okuda *et al* 1986, Joy and Vasudevan 1992, 1993) and nuclear magnetic resonance (Torre and Ziolo 1989). These authors have given estimates for the magnetic exchange between nearest neighbours both within and between planes. The results from these authors are not necessarily consistent. In addition, Pich and Schwabl (1995) have presented a theoretical calculation for the spin wave dispersion spectrum in isotropic two-dimensional honeycomb antiferromagnets. Thus it is the aim of this work to measure the spin wave dispersion curve and quantify the magnetic exchange integrals in $MnPS_3$.

The experimental technique required to unambiguously determine magnetic exchange integrals and spin wave dispersion is neutron inelastic scattering. Up until now it has been extremely difficult to do such experiments on this system because of the lack of single crystals of suitable size. The crystal used in this study was grown using a new technique, and was large enough for inelastic and diffuse neutron scattering experiments (Wildes *et al* 1998). The spin wave dispersion at 4 K has subsequently been measured and the exchange integrals were calculated by a least-squares fit to the data using linear spin wave theory.

Finally, as a prelude to further measurements on the critical scattering from this material the critical exponent of the magnetization below T_N, β, has been found by measuring the temperature dependence of the magnetic intensity of the (020) Bragg peak. This was

compared to the critical behaviour of the spin wave energy at the Brillouin zone centre as a function of temperature to ascertain the nature of the anisotropy.

2. The sample

Previously samples of this material have been prepared by a vapour deposition technique (Kurosawa *et al* 1983) or by direct heating of the base elements (Ouvrard *et al* 1985). These methods typically give powders, or platelike crystals large in two dimensions but very small in the third ($\approx 10 \times 10 \times 0.1$ mm^3). A new method was attempted to grow a crystal large enough for neutron scattering measurements.

The crystal was grown in a silica ampoule, approximately 120 mm in length and 15 mm internal diameter, with a conical tip. The ampoule was partially filled with a 1:1:3 ratio of Mn powder (4.524 g), P powder (2.551 g) and S flakes (7.923 g); all of 99.99% purity. All handling of the materials was performed under a dry N_2 atmosphere. The ampoule was pumped to 10^{-6} Torr, left overnight and then sealed. The ampoule was then loaded into a Bridgeman–Stockbarger resistive heated furnace controlled by a Eurotherm 900 EPC temperature controller. The upper zone was set to 900 °C and the lower zone to 635 °C, giving a nominal thermal gradient of 1 °C mm^{-1} and a temperature stability of ± 0.3 °C. The ampoule was lowered through these zones at 0.25 mm h^{-1} for 20 days. The furnace was then cooled to room temperature at 20 °C h^{-1}. A mass of crystals was obtained that had the green colour characteristic of $MnPS_3$. The best of these was $12 \times 10 \times 4$ mm^3, and was shown by x-ray Laue diffraction to be a single crystal with the $C2/m$ space group.

3. The experiments

Neutron scattering experiments on two separate instruments were necessary in order to measure the spin wave dispersion curve in $MnPS_3$. The instruments used were the IN14 and IN3 triple-axis spectrometers, both at the Institut Laue–Langevin, France.

IN14 is a cold neutron triple-axis spectrometer and as such it is optimized for measurements at small energy transfers. This instrument was used to measure the behaviour of the spin wave gap at the Brillouin zone centre as a function of temperature, the spin wave dispersion along the $[00\xi]$ direction where ξ is a reduced lattice unit and the spin wave dispersion along the $[0\xi 0]$ direction for $\xi < 0.5$. The monochromator and analyser were pyrolytic graphite, and a cooled beryllium filter was used between sample and analyser to filter high-order wavelengths. Collimators with $40'$ divergence were used between monochromator and sample, sample and analyser, analyser and detector. All measurements were carried out with the momentum transfer $\boldsymbol{Q}$ fixed, with k_I varying to measure energy transfers. The final neutron wave vector k_F was fixed between 1.1 and 1.5 Å^{-1} (2.507 and 4.662 meV respectively), the smaller k_F being necessary for high-resolution measurements.

Even with high resolution, scans close to the Brillouin zone centre reveal an asymmetric lineshape characteristic of the four-dimensional convolution of the dispersion surface with the resolution of the instrument. The spin wave energies were found in a least-squares fit procedure that correctly convoluted a fitted dispersion surface with the resolution volume by means of a Monte Carlo method. An example of the fit to the energy of the Brillouin zone centre is given in figure 2.

IN3 is a thermal neutron triple-axis spectrometer, and it was necessary to use this instrument to measure energy transfers greater than 5 meV. The spin wave dispersions along the $[0\xi 0]$ and $[\xi 00]$ directions were measured using this instrument.

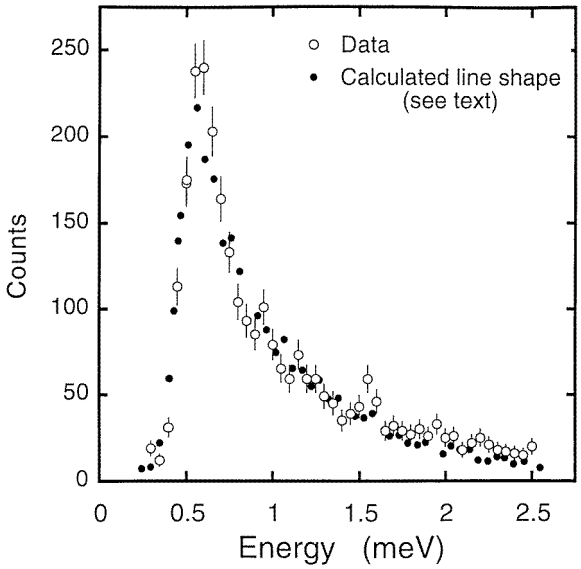

Figure 2. Fitted lineshape (filled circles) of the dispersion relation convoluted with the instrument resolution to the experimental data at the (020) position (open circles), temperature = 4 K. The fluctuations in the fit are due to statistics from the Monte Carlo routine.

A copper(111) monochromator and pyrolytic graphite(002) analyser were used, with higher-order wavelength contamination being filtered with pyrolytic graphite between sample and analyser. All measurements were carried out at constant $\boldsymbol{Q}$ and k_F fixed at 2.662 Å^{-1} (14.682 meV). When the spin wave dispersion had little gradient the measurements were carried out with no collimation and a horizontally curved analyser. Better Q resolution was required when the dispersion gradient was greater, and consequently these measurements were carried out using a flat analyser and with 40′ collimation between the sample and analyser, and between analyser and detector.

The measurements on IN3 were at points of the dispersion curve without pronounced $\boldsymbol{Q}$ dependence in the dispersion surface, and consequently it was sufficient to fit a Gaussian to the data to find the spin wave energy.

The intensity of the (020) Bragg peak was measured as a function of temperature on the TAS7 neutron triple-axis spectrometer at the DR3 reactor at Risø National Laboratory, Denmark. This is also a cold neutron spectrometer, and was used to measure elastic scattering. The monochromator was pyrolytic graphite. High-order wavelength contamination was filtered using cooled beryllium. Very coarse collimation divergence, 2°, was used before and after the sample. After careful alignment of the crystal using a pyrolytic graphite analyser, the analyser was removed and the (020) Bragg peak was measured at various temperatures by scanning along $[0\xi 0]$. The integrated intensity could then be calculated by trapezoidal summation and then subtracting an estimate for the background.

4. The spin wave dispersion

The measured spin wave dispersion spectrum is given in figure 3. The Brillouin zone and associated measurement directions are given in the inset of this figure.

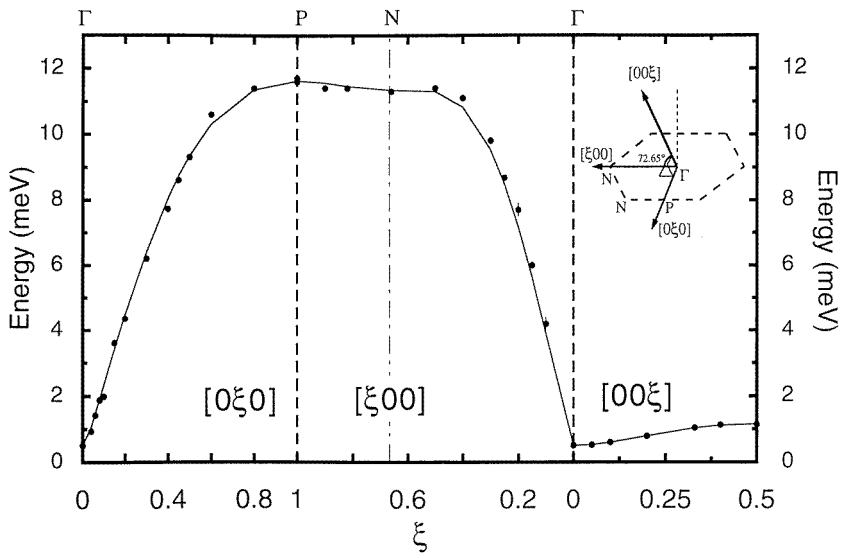

Figure 3. The spin wave dispersion in $MnPS_3$ along various high-symmetry directions. The directions in question are shown in the inset of the diagram.

The theoretical calculations of Pich and Schwabl (1995) predict a gap in the spin wave energy at the Brillouin zone centre of a magnitude $E_0 = 1.6$ meV and a splitting of the degeneracy of the spin wave branches, based on the hypothesis that a dipole–dipole interaction alone is responsible for the long-range magnetic ordering. As can be seen in the measured data, there is a small gap of magnitude $E_0 = 0.5$ meV and, to within the resolution of the measurement, there is no splitting in the degeneracy. There is also small dispersion along the [00ξ] direction. Thus, long-range magnetic ordering is more likely due to a combination of the magnetic exchange between the planes and whatever is responsible for the small anisotropy.

The dispersion can easily be fitted using the linear spin wave theory described by Keffer (1966). This theory accounts for anisotropy in the spin wave dispersion by introducing an easy-axis term $-g\mu_B H_A \sum_l S_l^z$ into the Hamiltonian, rather than the dipole–dipole interaction of Pich and Schwabl (1995). Inspection of the dispersion equations of Pich and Schwabl (Pich, private communication), however, reveals that for small anisotropy the dispersion relations calculated with the two Hamiltonians are approximately equivalent. The dispersion relation calculated by the method of Keffer is simpler, and consequently was the relation used to model the data.

To obtain reasonable agreement between calculated and measured dispersions it was necessary to include up to the third-nearest neighbours in the plane. In the absence of an external magnetic field the equation for $MnPS_3$ is

$$\begin{aligned} E_q^2 = {} & [g\mu_B H_A + 2S(6J_2 + 2J') - 2S(3J_1 + 3J_3) \\ & -2S\{J_2(2\cos(2\pi h) + 4\cos(\pi h)\cos(\pi k)) + 2J'\cos(2\pi l)\}]^2 \\ & -\left|2S\left\{J_1\left(\exp\left(-\frac{\mathrm{i}2\pi}{3}k\right) + 2\cos(\pi h)\exp\left(\frac{\mathrm{i}\pi}{3}k\right)\right)\right.\right. \\ & \left.\left. +J_3\left(\exp\left(\frac{\mathrm{i}4\pi}{3}k\right) + 2\cos(2\pi h)\exp\left(-\frac{\mathrm{i}2\pi}{3}k\right)\right)\right\}\right|^2. \end{aligned} \tag{1}$$

J_1, J_2 and J_3 are exchange integrals between first-, second- and third-nearest in-plane neighbours respectively and J' is the exchange between planes; h, k and l are the Miller indices of the scattering vector and H_A is the effective field due to anisotropy. This equation was then fitted to the data to obtain the values of J_{1-3} and J'. The fitted parameters are given in table 1.

Table 1. Values of the exchange integrals and the anisotropy in $MnPS_3$, as determined by the fit of equation (1) to figure 3.

S	J_1 (meV)	J_2 (meV)	J_3 (meV)	J' (meV)	$g\mu_B H_A$ (meV)
2.5	−0.77	−0.07	−0.18	0.0019	0.0086
	±0.09	±0.03	±0.01	±0.0002	±0.0009

Prior to this study, the value of the nearest-neighbour exchange J_1 had been estimated from magnetic susceptibility measurements. It has been calculated to be -0.82 ± 0.02 meV (Okuda *et al* 1986) and -0.78 meV (Joy and Vasudevan 1992) in analyses by molecular field theory, to be -0.70 meV in analysis by high-temperature series expansion (Joy and Vasudevan 1992, 1993) , and the magnitude to be 0.17 meV by nuclear magnetic resonance (Torre and Ziolo 1989). In mitigation, the last value should be considered an average over exchange integrals from further neighbours. Nevertheless, the spread in values is significant.

Likewise, the strength of the interlayer coupling and hence the validity of the approximation of two-dimensionality in this sample was subject to widely different estimates. Joy and Vasudevan (1993) have calculated the interlayer exchange constant $J' = 0.0013$ meV from a mean field treatment of the magnetic susceptibility with the ratio $|J'/J_1| = 0.0037$. This contrasts sharply with the ratio $|J'/J_1| \approx 0.4$ calculated from electron spin resonance measurements by Okuda *et al* (1986).

The measured J exchange integrals presented here agree well with some of the previously quoted values. J_1 is very close to one of the values stated by Joy and Vasudevan (1992). J' is very close to the value stated by the same authors (1993).

Rastelli *et al* (1979) have calculated in a mean-field approximation the values of the exchange integrals necessary for the stability of magnetic ordering in layered transition metal compounds at $T = 0$ K. Mean-field approximations are generally not applicable to two-dimensional materials. However, the authors state that a classical approximation will hold at very low temperatures, and any quantum effects will act to blur the predicted phase boundaries rather than refute the general validity of the theory. $MnPS_3$ has spin $5/2$ and is therefore more classical than quantum, and in addition the magnetic Bragg peak intensities as determined by neutron powder diffraction (Kurosawa *et al* 1983) may be fitted with a mean-field Brillouin function for $S = 5/2$. Consequently, the stability conditions of Rastelli *et al* (1979) can be applied.

The stability conditions for a honeycomb lattice with Heisenberg-like interactions and the magnetic structure of ordered $MnPS_3$ are:

$$J_3 \leqslant -J_1$$
$$2J_2 \geqslant J_1.$$

The values of J_{1-3} presented here are easily bounded by these inequalities, showing that the calculated exchange integrals are physical and consistent with the magnetic structure.

In addition, equations can be derived from mean-field theory to calculate the Néel temperature T_N and Curie point θ from the values of S and J_{1-3}. For $MnPS_3$ these equations

are:

$$\begin{aligned}\theta &= \tfrac{2}{3}S(S+1)(3J_1+6J_2+3J_3)/k_B \\ T_N &= \tfrac{2}{3}S(S+1)(-3J_1+6J_2-3J_3)/k_B.\end{aligned} \tag{2}$$

These equations give a value of $T_N = 164$ K and $\theta = -221$ K. Different authors have quoted the Curie point to be -230 ± 5 K (Okuda *et al* 1986), -220 K (Kurosawa *et al* 1983) and -160 K (Joy and Vasudevan 1992). The calculated Curie constant is very close to two of these three values. The calculated Néel temperature is approximately twice as large as the measured value. This is not surprising as the mean-field calculation of T_N is always too high for a material which exhibits strong critical fluctuations. Low-dimensional critical fluctuations are very strong in this material (Wildes *et al* 1998), and are the subject of further studies.

While the dispersion relations of Pich and Schwabl were not used to fit the data and are not necessary to accurately determine the exchange integrals, it is useful to return to them to ascertain the role of the dipole–dipole interaction in this material. An estimate of the strength of the dipole–dipole interaction may be extracted from their estimate for the magnitude of the spin wave gap:

$$E_0 = 2S[2(A_0^{zz} - \bar{A}_0^{zz} - A_0^{xx} + \bar{A}_0^{xx})|J|z]^{1/2} \tag{3}$$

where $|J|$ is the strength of the nearest-neighbour exchange, z is the number of nearest neighbours, $A_q^{\alpha\beta}$ is the Fourier transform of the dipole-dipole interaction between members of the *same* sublattice and $\bar{A}_q^{\alpha\beta}$ is the Fourier transform of the interaction *between* sublattices. The dipole–dipole interaction used in the calculation of Pich and Schwabl (1995) is:

$$A_{ll'}^{\alpha\beta} = \frac{1}{2}(g\mu_B)^2\left(\frac{3(\boldsymbol{x}_l - \boldsymbol{x}_{l'})_\alpha \cdot (\boldsymbol{x}_l - \boldsymbol{x}_{l'})_\beta}{|\boldsymbol{x}_l - \boldsymbol{x}_{l'}|^5} - \frac{\delta_{\alpha\beta}}{|\boldsymbol{x}_l - \boldsymbol{x}_{l'}|}\right). \tag{4}$$

In Fourier transforming equation (4) the magnitudes of $A_q^{\alpha\beta}$ and $\bar{A}_q^{\alpha\beta}$ are given by $(g\mu_B)^2$ multiplied by the appropriate summation over the lattice. This term is therefore the only free parameter in determining the strength of any dipole–dipole interaction. Using the measured E_0 and the calculated value for $|J|$ from table 1, this magnitude may be calculated from equation (3) to be $(g\mu_B)^2 = 0.0534$ meV Å^3, much smaller than that expected. Substitution of this value into the dispersion relations of Pich and Schwabl (Pich, private communication) verify that, to within instrumental resolution, no splitting would have been observed. Indeed, this calculation gives a dispersion identical to that of a similar calculation using equation (1) with an appropriate value of $g\mu_B H_A$. Thus, while the exchange integrals may be accurately determined from fitting an equation derived by linear spin wave theory to the measured dispersion, the nature of the anisotropy cannot.

In addition to their calculation of the expected spin wave dispersion curve, Pich and Schwabl (1995) also calculated the Néel temperature using the calculated strength of the dipole–dipole interaction and one of the previous estimates of the nearest-neighbour exchange interaction. The derived equation was given by $T_N \cong |J|/\ln(|J|/E_0)$, and for $|J| = 0.78$ meV the calculated value for the Néel temperature was $T_N = 73$ K, in agreement with the measured value of 78 K. When the current experimental values for $|J|$ and E_0 are substituted into this equation the calculation yields $T_N = 1.783$ meV $= 20.7$ K, well below the measured value. This suggests that the dipole–dipole interaction is not as important in stabilizing long-range ordering in this material as previously thought.

5. The critical behaviour below T_N, and the nature of the spin wave gap

One of the most direct methods of measuring the critical exponent of the magnetization, β, is by magnetic elastic scattering (Collins 1989). The magnetic Bragg peak intensity as measured by neutrons is proportional to the square of the perpendicular component of the magnetization to the scattering vector, i.e.

$$\frac{\mathrm{d}\sigma}{\mathrm{d}\Omega} \propto \langle M_{\perp}(\boldsymbol{Q})\rangle^2$$

where M is the magnetization, the angular brackets represent a configurational and thermal average and the subscript represents the perpendicular component of the magnetization to the scattering vector. The (020) peak is of particular interest because the magnetic scattering will be sensitive to the full magnetization, the direction of the magnetic moments being perpendicular to the scattering vector. The (020) magnetic Bragg peak intensity close to T_N will therefore vary with temperature according to the relation:

$$\frac{\mathrm{d}\sigma}{\mathrm{d}\Omega} = B_1\left[\frac{T_N - T}{T_N}\right]^{2\beta}. \tag{5}$$

The magnetic intensities as a function of temperature and the fit to equation (5) are shown in figure 4. The value of the critical exponent for the magnetization has been determined to be $\beta = 0.25 \pm 0.01$.

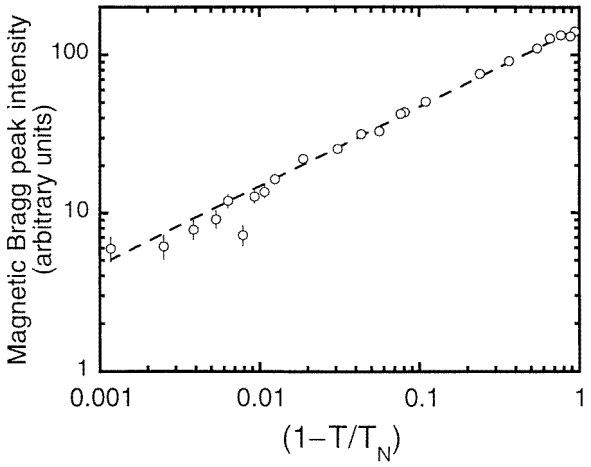

Figure 4. A log–log plot showing the magnetic Bragg peak intensity at the (020) position as a function of reduced temperature and the fit of equation (5) to the data. The slope of this line is 2β where β is the critical exponent of the magnetization.

It is interesting to note that this value is very close to the expected critical exponent from a 2D XY model, $\beta = 0.23$ (Bramwell and Holdsworth 1993), which suggests that the fluctuations are planar in character. This is somewhat surprising, as the moments point perpendicular to the ab planes which suggests a uniaxial anisotropy. There is, however, some further evidence to support planar fluctuations. Electron spin resonance measurements (Okuda *et al* 1986, Cleary *et al* 1986) show a small single-ion anisotropy that favours the spins to lie in the ab plane. Neutron powder diffraction above T_N has revealed broad peaks that were attributed to rodlike scattering in reciprocal space (Wildes *et al* 1994). While these rods have subsequently been shown to be due to critical fluctuations (Wildes *et al*

1998), comparisons of the peak heights showed the moments to be lying in the *ab* planes. Further critical scattering experiments are planned on this material to examine in more depth the nature of the fluctuations.

In an attempt to examine the nature of the anisotropy in this system the gap in the spin wave energies has also been measured as a function of temperature. All the magnetic Bragg peaks appear at existing nuclear Bragg peak positions. There is therefore some difficulty in measuring the spin wave gap at temperatures close to the Néel temperature, as the contamination caused by the nuclear Bragg peak makes measuring small energy transfers very difficult. As can be seen from figure 3 there is a very small dispersion along the [00ξ] direction. The spin wave gap was therefore measured at the reciprocal space position (0 2 0.05), at which point the energy of the spin waves is practically the same as that at the Brillouin zone centre.

A four-dimensional convolution of the resolution function with the spin wave dispersion surface was again attempted to determine the energy of the spin wave gap, and was reasonably successful for small temperatures. Unfortunately, close to the Néel temperature the peak in the inelastic scattering became lost in the resolution-broadened incoherent scattering, and consequently the fit results became unreasonable. As an approximation, the resolution was convoluted with an isotropic dispersion surface, and the incoherent component was approximated using a Gaussian. As the measurements are essentially at the Brillouin zone centre, the gradient of the spin waves was chosen to be small, approximately 0.5 meV $(\mathrm{rlu})^{-1}$. The scattering calculated using this approximation agreed reasonably well with the measured scattering. The spin wave gap could then be determined close to the Néel temperature by fitting the long 'tail' to the inelastic scattering.

What is sought in this analysis is an exponent similar and comparable to the critical exponent β determined above. The approximations detailed should make little difference to the determination of such an exponent, as any systematic errors in the fitting procedure will change the magnitude of the results but not the power-law behaviour. Comparison of the exponents calculated from the approximated fit to those of the more rigorous convolution with an anisotropic dispersion at low temperatures showed this to be the case.

The width of the inelastic scattering can also be used to investigate critical behaviour. Unfortunately the values for the widths returned from the fitting procedure proved unsatisfactory for this purpose. Although the shape of the scattering changes with temperature no distinction can be made between the temperature variation due to the broadening of the inelastic scattering and anisotropic temperature variation in the dispersion surface itself. It suffices to say that the calculated widths increase with increasing temperature, as is expected.

The gap in the spin wave energy calculated using the approximation is shown in figure 5, plotted against the reduced temperature. A power law was fitted to the data:

$$E_0 = B_2 \left[\frac{T_N - T}{T_N} \right]^c . \tag{6}$$

Inspection of figure 5 shows that there appear to be two values of c with a cross-over point at about $T = T_{cross} = 0.96\ T_N$. For $T < T_{cross}$ the exponent $c = 0.26 \pm 0.02$ compares favourably with β. For $T > T_{cross}$ the exponent $c = 0.51 \pm 0.02$ is double the value below T_{cross} and equal to the value of the exponent determined for the temperature behaviour of the magnetic Bragg peak intensity, 2β. It can therefore be said that the spin wave gap varies with the magnetisation below T_{cross}, and with the square of the magnetization above T_{cross}.

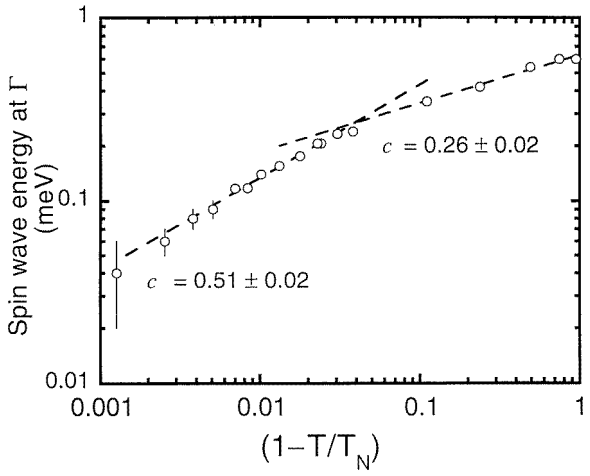

Figure 5. A log–log plot showing the spin wave energies at the Brillouin zone centre as a function of temperature and the fit of two power laws to the data. The exponent changes from $c = \beta$, where the gap varies as the magnetization, to $c = 2\beta$, where the gap varies as the squared magnetization, at temperature $T_{cross} = 0.96\ T_N$.

A variation of the spin wave gap with magnetization has been seen before in a variety of 2D materials, in particular square-lattice antiferromagnets, an excellent review of which is given by Arts and de Wijn (1990). Temperature dependence in the spin wave dispersion is attributed to interactions between spin waves, which may be taken into account in theory by expanding the spin operators to higher order. In this way, it is possible to show that in quadratic layer antiferromagnets the spin wave gap will vary with the magnetization both for a single-ion anisotropy (Nagata and Tomono 1974) and for dipole–dipole anisotropy (van Uijen and de Wijn 1984). While no such theories exists for honeycomb structures, it is reasonable to suggest that one is feasible. It is thus difficult to categorically state the nature of the anisotropy in $MnPS_3$ based on the low-temperature behaviour of the spin wave gap.

A variation of the spin wave gap with the squared magnetization is less common in low dimensions, although this effect has been seen in another 2D $S = 5/2$ system, $KFeF_4$ (Fulton *et al* 1994). At this point there appears to be no theory to explain this.

A change in the behaviour of the spin wave gap is not unprecedented, nor is it outside the scope of current theories. Both the theories of Nagata and Tomono (1974) and van Uijen and de Wijn (1984) collapse for $T > 0.5\ T_N$, above which temperature magnon–magnon interactions become increasingly important. Okuda *et al* (1986) have reported both single-ion and dipolar anisotropies of comparable magnitude in $MnPS_3$ based on antiferromagnetic resonance measurements at 4.2 K and considered the resultant anisotropy to be due to a competition between these two effects. Keffer (1966) has summarized the classical theories to predict the effect of temperature on anisotropy, showing a power-law relation between the anisotropy and the magnetization. While the exponents calculated by these theories do not match those observed in this study, it can be shown that the variation of the anisotropy with magnetization can change with temperature, and that this temperature dependence depends on the nature of the anisotropy. It is therefore possible that the observed behaviour of the spin wave gap reflects the competition between the two anisotropies, which may have different temperature dependence and which may influence the nature of magnon–magnon interactions at temperatures close to T_N, resulting in the observed cross-over.

A second possibility is suggested by the critical exponent of the magnetization, which as mentioned above appears to fit in to an XY-like universality class. True XY systems should show a 'Kosterlitz–Thouless' phase transition (Kosterlitz and Thouless 1973) at a temperature T_{KT}. In a quasi-2D XY system there will be some transition to long-range 3D ordering at a temperature slightly higher than T_{KT} due to finite interplanar coupling (Regnault and Rossat-Mignod 1990 and references therein). In such systems, at temperatures close to T_{KT} the magnetization is expected to drop steeply with temperature and a discontinuous decrease is expected in the spin wave gap. Such behaviour has been seen in a quasi-2D XY material with a honeycomb magnetic structure, $BaNi_2(PO_4)_2$ (Regnault and Rossat-Mignod 1990). It is true that in $MnPS_3$ the variation of magnetization with temperature is constant over the entire temperature range; however it may be possible that T_{cross} indicates a cross-over to excitations of a Kosterlitz–Thouless nature. Further critical scattering measurements of the excitations in this system are planned to investigate this question further.

6. Conclusions

The spin wave dispersion spectrum has been measured in $MnPS_3$, and could easily be modelled with linear spin wave theory if the equation included exchange interactions up to the third-nearest neighbour in the plane. The values of the exchange integrals correspond with those determined by previous authors using other methods. A spin wave gap was detected at the Brillouin zone centre, and this was measured as a function of temperature up to the Néel point. It was found to decrease with the magnetization far from T_N, and to decrease with magnetization squared close to T_N, although the reason for this is not certain. The critical exponent of the magnetization was determined to be $\beta = 0.25 \pm 0.01$.

Acknowledgments

The authors would like to thank the ILL for the use of the IN14 and IN3 spectrometers, the EC-TMR access to large-scale facilities programme for the use of TAS7 at Risø National Laboratory and the Clarendon Laboratory for the use of their crystal growing facilities. Thanks also to Professor R A Cowley, Dr D A Tennant and Dr C Pich for their valuable comments, and Dr M Zolliker, Mr P Decarpentrie and Mr A Brochier for their assistance in the course of the experiments. This work was funded by the EPSRC.

References

Arts A F M and de Wijn H W 1990 *Magnetic Properties of Layered Transition Metal Compounds* ed L J de Jongh (Deventer: Kluwer) p 191
Bramwell S T and Holdsworth P C W 1993 *J. Phys.: Condens. Matter* **5** L53
Cleary D A, Francis A H and Lifshitz E 1986 *Chem. Phys.* **106** 123
Collins M F 1989 *Magnetic Critical Scattering* (Oxford: Oxford University Press)
Fulton S, Nagler S E, Needham L M N and Wanklyn B M 1994 *J. Phys.: Condens. Matter* **6** 6667
Joy P A and Vasudevan S 1992 *Phys. Rev.* B **46** 5425
——1993 *J. Chem. Phys.* **99** 4411
Keffer F 1966 *Handbuch der Physik* vol 18II (Berlin: Springer)
Kosterlitz J M and Thouless D J 1973 *J. Phys. C: Solid State Phys.* **6** 1181
Kurosawa K, Saito S and Yamaguchi Y 1983 *J. Phys. Soc. Japan* **52** 3919
Nagata K and Tomono Y 1974 *J. Phys. Soc. Japan* **36** 78
Okuda K, Kurosawa K, Saito S, Honda M, Zhihong Y and Date M 1986 *J. Phys. Soc. Japan* **55** 4456

Ouvrard G, Brec R and Rouxel J 1985 *Mater. Res. Bull.* **20** 1181
Pich C and Schwabl F 1995 *J. Magn. Magn. Mater.* **148** 30
Rastelli E, Tassi A and Reatto L 1979 *Physica* B **97** 1
Regnault L P and Rossat-Mignod J 1990 *Magnetic Properties of Layered Transition Metal Compounds* ed L J de Jongh (Deventer: Kluwer) p 271
Torre S and Ziolo J 1989 *Phys. Rev.* B **39** 8915
van Uijen C M J and de Wijn H W 1984 *Phys. Rev.* B **30** 5265
Wildes A R, Harris M J and Godfrey K W 1998 *J. Magn. Magn. Mater.* **177–181** 143
Wildes A R, Kennedy S J and Hicks T J 1994 *J. Phys.: Condens. Matter* **6** L335